Results of a MIMO Testbed with Geosynchronous Ku-Band Satellites

Robert T. Schwarz, Christian Hofmann, and Andreas Knopp
Chair of Signal Processing
Munich University of the Bundeswehr, 85579 Neubiberg, Germany
Email: papers.sp@unibw.de

***Abstract*—If multiple-input multiple-output (MIMO) satellite communications (SATCOM) systems use spatial multiplexing, the channel capacity depends on the geometrical conditions of the antenna setup. This theoretical result is proven and confirmed for the first time by a true-MIMO test campaign. To this end, we utilize two Ku-band satellites and a ground station with two antennas as a 2×2 MIMO SATCOM measurement system. The channel capacity is estimated and compared to its theoretical prediction. The probing results show a perfect match to the theoretical predictions.**

I. Introduction

Due to their potentially high bandwidth efficiency, multiple-input multiple-output (MIMO) systems are an integral part of today's terrestrial wireless communications standards. In SATCOM, however, the applicability of the MIMO technology with spatially distributed antenna elements is subject to contentious discussions in the scientific community [1]. The main reason can be found in the characteristics of the SATCOM channel. The satellite channel for Fixed Satellite Services (FSS) or Mobile Satellite Services (MSS) in frequency bands above 10 GHz is specified by a strong Line-of-Sight (LOS) signal with no or negligible multipath components (MPC), where MPC are widely believed to be a prerequisite for high MIMO gains.

On the other hand, it has already been shown by theory that high MIMO gains in strong LOS channels are possible, if particular antenna geometries are considered. This idea has been applied to SATCOM in [2], and a criterion has been developed for the optimal positioning of the MIMO antenna elements on Earth and in geostationary earth orbit (GEO). It has been shown that the inter-antenna spacing is a key parameter, but comparably large separations are required either on Earth or in orbit. This leads to mainly two concepts: a) multiple antennas onboard a single-satellite, or b) multiple satellites at different orbit positions.

This paper is dedicated to prove for the first time the theoretical results provided in [2] by means of real satellite channel measurements. More precisely, we will probe the MIMO channel with an appropriate training sequence that gives us the channel capacity in return. To this end we have developed a measurement system comprising two transmitter (Tx) antennas and two receiver (Rx) antennas on Earth. A single-satellite with two antennas and overlapping service zones in up- and downlink and in the same frequency bands is not available yet. Therefore, we have developed a special setup that provides us with a MIMO channel formed by two existing satellites working in the same frequency band. We utilize the two satellites "EUTELSAT 7B" (E7B) and "EUTELSAT 10A" (E10A), which have a small frequency range in common, provide an overlapping downlink coverage, and are only 3° apart. We use small Rx antennas with a wide main lobe so that both satellites can be received simultaneously when the Rx antennas point directly between E7B and E10A. An adjustable Rx antenna separation on ground enables us to probe the influence of the antenna geometry on the channel capacity.

The conducted SATCOM measurement campaign with spatially distributed antenna elements on ground and in orbit is the first of its kind. We consider the results as a breakthrough towards future MIMO SATCOM implementations since the achievable MIMO capacity has now been practically determined and validated. The probing results will prove very impressively that carefully placed antenna elements lead to the maximum channel capacity in MIMO SATCOM applications. Thus, seven years of its original publication at the Workshop on Smart Antennas (WSA) 2008 in Darmstadt, Germany, we will now report on the practical "proof of concept" of this innovative approach.

Please note that the focus of this paper is thus on the proof of the theoretical predictions in [2] regarding the dependence of the MIMO channel capacity on the geometrical antenna arrangement in LOS SATCOM channels. Hence, the described MIMO measurement system fulfills the specific needs to proof the theory. It is therefore not intended to provide an economically meaningful MIMO SATCOM system proposal for practically relevant use cases. Moreover, the applicability of other MIMO concepts, e.g. exploiting the polarization domain than the spatial domain, are not part of this paper. Also typical and already known issues encountered when trying to realize a spatial MIMO SATCOM system, like for example different propagation delays on the MIMO paths [3], will not be discussed here and needs to be addressed in future works.

The rest of the paper is organized as follows: Section II gives an overview of the probing testbed and describes its main technical characteristics. Section III contains the theoretical background on the considered LOS MIMO channel and the capacity calculation. Section IV describes briefly the estimation approach we have applied. The probing results are discussed in section V and an estimate of the error induced by

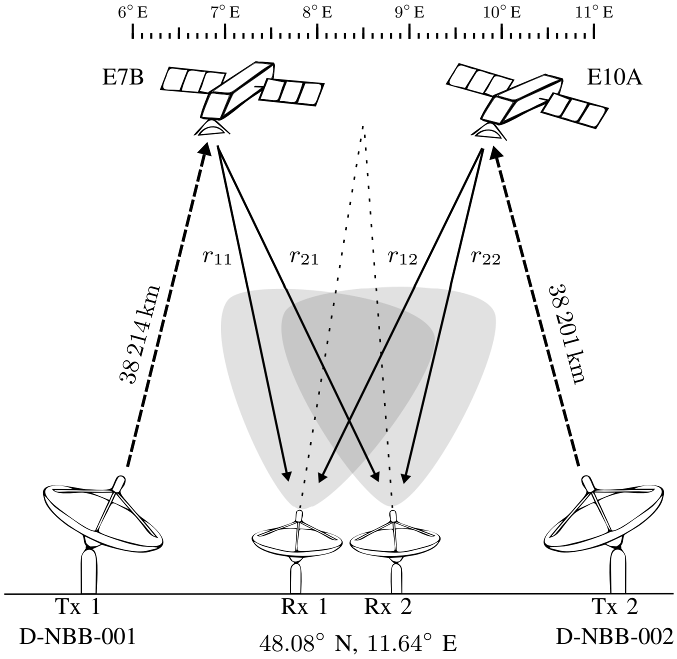

Fig. 1. Overview of the measurement system and setup.

measurement uncertainties is provided, before we conclude in section VI.

II. Overview of the Measurement System

The MIMO satellite measurement system consists of two Tx terminals, two Rx terminals and two GEO satellites. Fig. 1 shows a graphical illustration of the setup. We have used leased capacity on the two GEO satellites E7B and E10A at 7° East and 10° East, respectively. Both satellites provide transparent payloads and share a small part of the Ku-band spectrum in up- and downlink. In particular the up- and downlink center frequencies have been $14.005\,\mathrm{GHz}$ and $12.505\,\mathrm{GHz}$, respectively, with an available bandwidth of $500\,\mathrm{kHz}$ on both satellites, sufficiently large to perform the measurements. They are equipped with linearized traveling wave tube amplifiers (TWTAs) and are operated in the linear regime. Tx and Rx are both located at $48.08°$ North and $11.64°$ East, which is on the roof top of our laboratory building in Neubiberg, Germany. A photography of the Tx and Rx antenna farm is shown in fig. 2.

The Tx antennas are $1.8\,\mathrm{m}$ dishes providing a maximum equivalent isotropically radiated power (EIRP) of $55.7\,\mathrm{dBW}$ each at $14\,\mathrm{GHz}$. They act as two single-input single-output (SISO) feeder uplinks, one for each satellite, i.e. Tx antenna 1 points towards E7B, and Tx antenna 2 points towards E10A.

The downlink forms a 2×2 MIMO channel with two elliptical aperture dishes with $0.75\,\mathrm{m}$ equivalent diameter, having a $3\,\mathrm{dB}$-beamwidth of approximately $2.0°$ at $12\,\mathrm{GHz}$ each. Both Rx dishes point at the geostationary arc at longitude $8.5°$ East, i.e. exactly between E7B and E10A so that both downlink signals can be received by each Rx antenna simultaneously via the edges of the main lobe. As

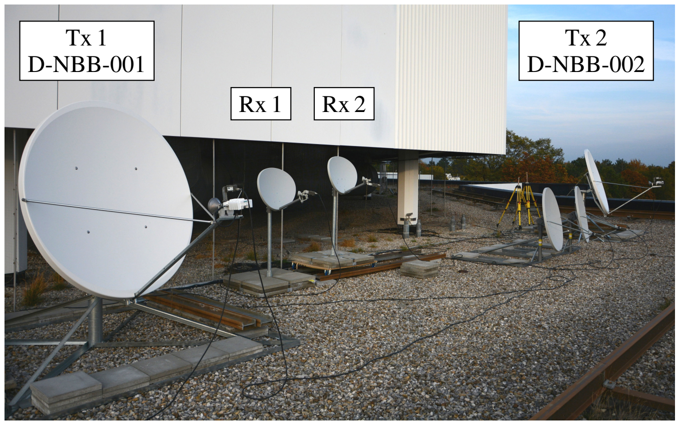

Fig. 2. Photography of the antenna farm showing the Tx and Rx antennas of the MIMO SATCOM measurement system.

a consequence we have to cope with a gain fall out of approximately $-12\,(1.5°/2.0°)^2 = -6.8\,\mathrm{dB}$[1]. The resulting effective figure of merit (G/T) towards each satellite is approximately $17.3\,\mathrm{dB/K} - 6.8\,\mathrm{dB} = 10.5\,\mathrm{dB/K}$, which is sufficiently high to obtain reliable measurement results. Moreover, to estimate the MIMO capacity as a function of the antenna geometry, Rx antenna 2 is moveable on a bar (please refer to fig. 2). Thus, the inter-antenna distance d between both Rx antennas can be adjusted along a fine grid within a range of $1.4\,\mathrm{m}$ to $3.7\,\mathrm{m}$.

All ground components run with a common $10\,\mathrm{MHz}$ reference clock from one Rubidium oscillator and are, thus, perfectly synchronized in frequency and time. Due to free running oscillators in the satellites and independent movements of both satellites within their station keeping box, a carrier frequency offset between both receive signals at Rx 1 and Rx 2 needs to be considered. This carrier frequency offset has been estimated before each channel access by comparison of the center frequencies at Rx 1 and Rx 2. Through individual and appropriate tuning of each uplink center frequency at Tx 1 and Tx 2 this carrier offset has been compensated successfully.

III. Channel Model and Capacity Calculation

In this section we introduce the theoretical background in terms of the considered satellite channel model and related capacity calculations. The probing results provided in the following sections will show that these theoretical considerations perfectly match in practice.

A. *MIMO Satellite Channel Model*

We consider a 2×2 MIMO SATCOM downlink channel in the following. The system bandwidth in SATCOM applications above $10\,\mathrm{GHz}$ is usually much smaller than the carrier frequency [4]. In that case the satellite channel is a frequency flat fading LOS channel, which has also been proven through

[1]Please note, that this calculation is only valid for sufficiently small off-axis angles, i.e. typically smaller than half the $3\,\mathrm{dB}$-beamwidth [4]. Although this is not fulfilled in our measurement setup this value is sufficient to get a rough estimate for the link budget. The estimate is sufficient for the analysis presented in this paper.

channel measurements in [5]. The LOS channel coefficient H_{mn} between the n-th Tx and the m-th Rx antenna can be modeled in complex baseband as[2]

$$H_{mn} = a_{mn} \exp\{-\mathrm{j}\,\vartheta_{mn}\} = a_{mn} \exp\left\{-\mathrm{j}\,\frac{2\pi}{\lambda_c} r_{mn}\right\}. \quad (1)$$

Here, λ_c is the wavelength at the downlink center frequency, i.e. $\lambda_c = c_0/f_c$ with c_0 being the speed of light in free space. r_{mn} is the path length between the m-th Rx antenna on the ground and the n-th satellite. The amplitude a_{mn} is modeled according to the free space wave propagation mechanism as

$$a_{mn} = \frac{\lambda_c}{4\pi r_{mn}} \approx a = \text{const.}\,\forall\, m, n \quad (2)$$

The above approximation is very reasonable since the different path lengths r_{mn} are nearly identical with only small variations compared to its mean total length.

We define the 2×2 channel transfer matrix (CTM) $\boldsymbol{H}$ containing the four LOS channel coefficients H_{mn}, and write

$$\boldsymbol{H} = a \cdot \boldsymbol{H}_{\text{norm}}, \quad (3)$$

where $\boldsymbol{H}_{\text{norm}}$ denotes the normalized CTM containing only the phase entries according to

$$[\boldsymbol{H}_{\text{norm}}]_{m,n} = \exp\{-\mathrm{j}\,\vartheta_{mn}\}. \quad (4)$$

B. MIMO Channel Capacity

The MIMO spectral efficiency with arbitrary and equally probable transmit symbols as channel inputs, and in case of additive white Gaussian noise (AWGN) is calculated according to [6]

$$\mathcal{C} = \log_2\left(\det\left(\boldsymbol{I} + \rho^{(\text{ref})} \cdot \boldsymbol{H}_{\text{norm}} \boldsymbol{H}_{\text{norm}}^{\text{H}}\right)\right), \quad (5)$$

where $\rho^{(\text{ref})}$ is the reference signal-to-noise ratio (SNR) at the receiver input. Please note that we incorporate the path loss of the channel into $\rho^{(\text{ref})}$ and need to use the normalized CTM $\boldsymbol{H}_{\text{norm}}$ instead of $\boldsymbol{H}$ in (5). The SNR at the receiver input is then written as

$$\rho^{(\text{ref})} = \frac{P_T\,|a|^2}{\sigma_{\boldsymbol{\eta}}^2}, \quad (6)$$

where P_T stands for the radiated signal power per satellite, which is assumed to be equal for both satellites of the considered system. We also assume equal noise powers $\sigma_{\boldsymbol{\eta}}^2$ at each receive antenna in this model. Moreover, the noise is AWGN and uncorrelated in space and time.

The MIMO channel capacity is maximized for orthogonal MIMO channels and minimized in the case of the so-called keyhole channel. Examples with the dimension 2×2 of an orthogonal and a keyhole MIMO channel are

$$\boldsymbol{H}_{\text{norm}}^{(\text{opt})} = \sqrt{2}\boldsymbol{I}, \text{ and } \boldsymbol{H}_{\text{norm}}^{(\text{key})} = \mathbf{1}, \text{ respectively,} \quad (7)$$

where $\mathbf{1}$ is a matrix containing 1 in all entries. The maximum channel capacity of a 2×2 MIMO channel is given by [6]

$$\mathcal{C}_{\text{opt}} = 2 \cdot \log_2\left(1 + \rho^{(\text{ref})} \cdot 2\right). \quad (8)$$

It has been shown by theory that in strong LOS channels distinct geometrical arrangements between the Rx and Tx antenna elements are the key to obtain orthogonal channels with maximum capacity. This has been applied in [2] to derive a general optimization criterion for orthogonal LOS MIMO channels. For a 2×2 channel the geometrical criterion writes

$$r_{21} - r_{22} + r_{12} - r_{11} = v\frac{\lambda_c}{2}, v \in \mathbb{Z}, v \nmid 2. \quad (9)$$

v is an integer and can be chosen arbitrarily in $\mathbb{Z}$ but must be indivisible by 2, i.e. $v \nmid 2$. Applying the geographical parameters of our measurement setup from fig. 1, condition (9) delivers an optimal spacing of the Rx antennas of[3]

$$d_{\text{opt}} = v \cdot 21.7\,\text{cm}. \quad (10)$$

Odd multiples of this optimal inter-antenna spacing on Earth result in an orthogonal MIMO downlink channel as the measurement results will show in the sequel.

IV. Channel Estimation

The objective of the MIMO satellite measurement system briefly described in section II is to estimate the four channel coefficients H_{mn} of the downlink for various geometrical antenna configurations. The channel capacity can then be calculated and will be compared to the theoretical values when applying the model above.

To estimate the MIMO SATCOM channel we utilize a constant amplitude zero autocorrelation (CAZAC) sequence, which is a complex-valued pseudo-noise sequence with constant modulus. It offers perfect noise-like autocorrelation properties. In particular, the used training sequence in discrete time is of the form [7]

$$c[n] = \exp\left\{\mathrm{j}\,\frac{K_c \pi n^2}{L_c}\right\} \quad (11)$$

with length $L_c = 1000$, $n = 0, \ldots, L_c - 1$ and $K_c = 1$. Doppler effects due to independent satellite movements have been estimated in advance of each measurement cycle and resulting frequency offsets have been corrected.

Using the CAZAC sequence, the channel coefficients are estimated employing a Best Linear Unbiased Estimator (BLUE) [8]. For a thorough mathematical description of the performed estimation the reader is kindly referred to [9] and [5]. The BLUE implements a linear maximum-likelihood estimation in the case of AWGN and meets the Cramer-Rao-Bound. Thus, using a BLUE provides us with otpimal estimation result [8]. We denote the estimated CTM as $\hat{\boldsymbol{H}}$ containing the estimated channel coefficients $\hat{H}_{mn} = \hat{a}_{mn} \exp\left\{-\mathrm{j}\,\hat{\vartheta}_{mn}\right\}$.

The measurement SNR $\rho^{(\text{meas})}$ has been approximately between 3 dB and 4 dB at Rx antenna 1 and Rx antenna 2, respectively. Slightly different values between both Rx antennas

[2]In this paper the following mathematical notations are applied: $\mathrm{E}\{.\}$ is the expectation operator over all possible realizations of a random variable. $\det(.)$ is the determinant of a matrix. $(.)^{\text{H}}$ and $(.)^{\text{T}}$ is the conjugate transpose and the transpose of a matrix or a vector, respectively, and $\sqrt{-1} = \mathrm{j}$. $\boldsymbol{I}$ is the identity matrix of appropriate dimension.

[3]To calculate this value eq. (22) in [2] has been applied.

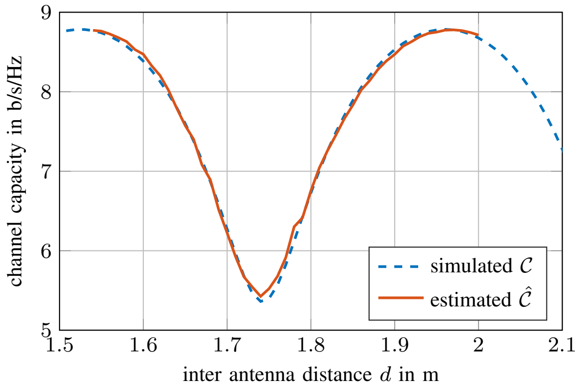

Fig. 3. Capacity estimation of the measured MIMO SATCOM channel and comparison with simulation results, assumed $\rho^{(\mathrm{ref})}$ of 10 dB.

$\rho^{(\mathrm{meas})}$	5 dB	10 dB	33 dB
$\mu_{\hat{\mathcal{C}}}$	8.9 b/s/Hz	8.8 b/s/Hz	8.8 b/s/Hz
$\sigma_{\hat{\mathcal{C}}}$	1.12 b/s/Hz	0.62 b/s/Hz	0.04 b/s/Hz
$\sigma^2_{\hat{\mathcal{C}}}$	1.25 (b/s/Hz)^2	0.38 (b/s/Hz)^2	0.002 (b/s/Hz)^2

TABLE I

SIMULATION RESULTS TO INVESTIGATE THE ESTIMATION ERROR: MEAN $\mu_{\hat{\mathcal{C}}}$, STANDARD DEVIATION $\sigma_{\hat{\mathcal{C}}}$ AND VARIANCE $\sigma^2_{\hat{\mathcal{C}}}$ OF ESTIMATED $\hat{\mathcal{C}}$, THREE MEASUREMENT SNRS $\rho^{(\mathrm{MEAS})}$, ORTHOGONAL CHANNEL $\boldsymbol{H}^{(\mathrm{opt})}_{\mathrm{NORM}}$

$\rho^{(\mathrm{meas})}$	5 dB	10 dB	33 dB
$\mu_{\hat{\mathcal{C}}}$	7.3 b/s/Hz	6.3 b/s/Hz	5.4 b/s/Hz
$\sigma_{\hat{\mathcal{C}}}$	1.09 b/s/Hz	0.68 b/s/Hz	0.02 b/s/Hz
$\sigma^2_{\hat{\mathcal{C}}}$	1.18 (b/s/Hz)^2	0.46 (b/s/Hz)^2	0.0005 (b/s/Hz)^2

TABLE II

SIMULATION RESULTS TO INVESTIGATE THE ESTIMATION ERROR: MEAN $\mu_{\hat{\mathcal{C}}}$, STANDARD DEVIATION $\sigma_{\hat{\mathcal{C}}}$ AND VARIANCE $\sigma^2_{\hat{\mathcal{C}}}$ OF ESTIMATED $\hat{\mathcal{C}}$, THREE MEASUREMENT SNRS $\rho^{(\mathrm{MEAS})}$, KEYHOLE CHANNEL $\boldsymbol{H}^{(\mathrm{key})}_{\mathrm{NORM}}$

are the result of small pointing inaccuracies of the 0.75 m Rx dishes towards 8.5° East. However, the exact SNR values are not important for the estimation accuracy since we obtain a remarkable correlation gain from the CAZAC sequence. The maximum improvement of the measurement SNR depends on the length L_c, which is $10 \cdot \log_{10}(L_c) = 30\,\mathrm{dB}$ in our case. Thus, we finally achieve values for the measurement SNR $\rho^{(\mathrm{meas})}$ between 33 dB and 34 dB. This measurement SNR is sufficient to obtain reliable estimation results as shown by the error analysis in the sequel.

V. Probing Results

A. Estimated Channel Capacity

Analog to (5), the estimated channel capacity $\hat{\mathcal{C}}$ at any reference SNR can be calculated using the measured normalized channel transfer matrix $\hat{\boldsymbol{H}}_{\mathrm{norm}}$ according to

$$\hat{\mathcal{C}} = \log_2\left(\det\left(\boldsymbol{I} + \rho^{(\mathrm{ref})} \cdot \hat{\boldsymbol{H}}_{\mathrm{norm}}\hat{\boldsymbol{H}}^{\mathrm{H}}_{\mathrm{norm}}\right)\right) \tag{12}$$

To verify the dependence of the capacity on the antenna geometry we measured the MIMO SATCOM channel for different Rx antenna separations. The result is given in fig. 3 showing the estimated capacity $\hat{\mathcal{C}}$ according to (12) as a function of d. The inter-antenna spacing d has been adjusted in steps of 1 cm by hand, starting with approximately $d_{\mathrm{opt}} = 7 \cdot 21.7\,\mathrm{cm} = 1.52\,\mathrm{m}$. To compare $\hat{\mathcal{C}}$ derived from measurements with our theoretical predictions, the theoretical LOS MIMO channel $\boldsymbol{H}_{\mathrm{norm}}$ has been calculated using the known real antenna and satellite positions. With $\boldsymbol{H}_{\mathrm{norm}}$ the exact capacity $\mathcal{C}$ according to (5) has been calculated and is shown in the figure for comparison.

The probing results match very well the theoretical simulations. The curves in fig. 3 prove the predicted dependence of the channel capacity on the antenna geometry very exactly. However, comparing $\hat{\mathcal{C}}$ with $\mathcal{C}$ the keyhole capacity of $\hat{\mathcal{C}}$ is slightly increased. The reason will be discussed in the following.

B. Estimation Error Analysis

The estimation error $\triangle\hat{H}$ in $\hat{\boldsymbol{H}}_{\mathrm{norm}}$ leads to an error in $\hat{\mathcal{C}}$ as well. In [10] it has been shown that the erroneous CTM $\hat{\boldsymbol{H}}_{\mathrm{norm}}$ with respect to noise can be analyzed by computer simulation if we use

$$\hat{\boldsymbol{H}}_{\mathrm{norm}} = \boldsymbol{H}_{\mathrm{norm}} + 1/\sqrt{\rho^{(\mathrm{meas})}}\boldsymbol{G}. \tag{13}$$

$\boldsymbol{G}$ is a matrix with independent complex Gaussian distributed random entries with unity variance and $\rho^{(\mathrm{meas})}$ is the measurement SNR considered. Using (13) in (12) the effect of the estimation error on $\hat{\mathcal{C}}$ in terms of the measurement SNR $\rho^{(\mathrm{meas})}$ can be analyzed. Several realizations of $\boldsymbol{G}$ for different measurement SNR $\rho^{(\mathrm{meas})}$ and fixed SNR $\rho^{(\mathrm{ref})} = 10\,\mathrm{dB}$ have been simulated. Moreover, we considered two 2×2 cases for $\boldsymbol{H}_{\mathrm{norm}}$ in (13), the keyhole channel $\boldsymbol{H}^{(\mathrm{key})}_{\mathrm{norm}}$ and an orthogonal channel $\boldsymbol{H}^{(\mathrm{opt})}_{\mathrm{norm}}$. The results of this Monte Carlo simulation in terms of the mean values $\mu_{\hat{\mathcal{C}}}$, the standard deviations $\sigma_{\hat{\mathcal{C}}}$ and the variances $\sigma^2_{\hat{\mathcal{C}}}$ of the estimated capacities $\hat{\mathcal{C}}$ for the different cases are given in tab. I for the orthogonal channel, and in tab. II for the keyhole channel. Please note that the exact capacity values at $\rho^{(\mathrm{ref})} = 10\,\mathrm{dB}$ are $\mathcal{C}\left(\boldsymbol{H}^{(\mathrm{key})}_{\mathrm{norm}}\right) = 5.4\,\mathrm{b/s/Hz}$ in the case of the keyhole channel, and $\mathcal{C}\left(\boldsymbol{H}^{(\mathrm{opt})}_{\mathrm{norm}}\right) = 8.8\,\mathrm{b/s/Hz}$ in the case of the orthogonal channel.

While the mean estimation error can be neglected in the case of an orthogonal channel, the additive noise from $\rho^{(\mathrm{meas})}$ leads to an overestimation of the actual capacity in the case of the keyhole channel. This is due to the excitation of the eigenmodes that the true channel would not excite [10]. In other words, while the pure LOS channel in the keyhole case adopts identical phase values for each CTM entry, the AWGN adds arbitrary and statistically independent phases per matrix entry. The arbitrary phase contributions increase if the noise power increases compared to the signal power. However, since arbitrary and statistically independent channel matrix entries result in a high ergodic channel capacity, as it is for example known for Rayleigh channels, additive noise leads to an overestimation of the ergodic (or mean) channel capacity. This can be observed from the first line of tab. II, where the mean values $\mu_{\hat{C}}$ are given for the three exemplary measurement SNRs. The only way to combat this effect is a sufficiently high measurement SNR, which has been achieved in our measurements. For $\rho^{(\text{meas})} = 33\,\text{dB}$, the mean values $\mu_{\hat{C}}$ coincide with the exact values of $8.8\,\text{b/s/Hz}$ and $5.4\,\text{b/s/Hz}$ in both cases, the orthogonal MIMO channel and the keyhole channel. The very small standard deviations of only $0.04\,\text{b/s/Hz}$ and, respectively, $0.02\,\text{b/s/Hz}$ prove the reliability of the estimates.

Moreover, the reference SNR $\rho^{(\text{ref})}$ for the capacity estimation should always be lower than the measurement SNR $\rho^{(\text{meas})}$ in order to obtain reliable estimation results [10]. To sum up, the results in both tables reveal that in our particular case, i.e. a measurement SNR $\rho^{(\text{meas})}$ of about $33\,\text{dB}$ and an assumed reference SNR of $10\,\text{dB}$, estimation errors in $\hat{C}$ can be neglected.

VI. Conclusion

In this paper we have presented the results of a multiple-input multiple-output (MIMO) satellite channel measurement campaign. The measurement system consists of two transmit antennas, two receive antennas and two geostationary satellites at different orbit positions having an orbital separation of $3°$. Our objective has been to estimate the practically achievable channel capacity in spatial MIMO satellite applications operating in frequency bands above $10\,\text{GHz}$. Moreover, we aim to prove previous theoretical analysis that promise maximum MIMO gains for SATCOM systems. Our probing results have shown very impressively that the maximum MIMO capacity can be achieved in practice through carefully placed antenna elements. As this is the first practical prove of the capacity gains offered by spatially optimized antenna setups, we consider the results as breakthrough in in MIMO satellite communications.

References

[1] P.-D. Arapoglou, K. Liolis, M. Bertinelli, A. Panagopoulos, P. Cottis, and R. D. Gaudenzi, "MIMO over Satellite: A Review," *Communications Surveys Tutorials, IEEE*, vol. 13, no. 1, pp. 27–51, 2011.

[2] R. Schwarz, A. Knopp, D. Ogermann, C. Hofmann, and B. Lankl, "Optimum-capacity MIMO satellite link for fixed and mobile services," in *Smart Antennas, 2008. WSA 2008. International ITG Workshop on*, Feb 2008, pp. 209–216.

[3] R. Schwarz, A. Knopp, and B. Lankl, "Performance of an SC-FDE SATCOM System in Block-Time-Invariant Orthogonal MIMO Channels," in *Global Telecommunications Conference (GLOBECOM 2011), 2011 IEEE*, Dec 2011, pp. 1–6.

[4] G. Maral and M. Bousquet, *Satellite Communications Systems: Systems, Techniques and Technology*, 5th ed. John Wiley & Sons, Dec. 2009.

[5] C. A. Hofmann, R. T. Schwarz, R. T. Schwarz, and A. Knopp, "SOTM Measurements for the Characterization of the Wideband Mobile Satellite Channel at Ku-Band," in *SCC 2015; 10th International ITG Conference on Systems, Communications and Coding; Proceedings of*, Feb 2015, pp. 1–8.

[6] I. E. Telatar, "Capacity of Multi-antenna Gaussian Channels," *European Transactions on Telecommunications*, vol. 10, no. 6, pp. 585–595, Nov. 1999, Technical Memorandum, Bell Laboratories, Lucent Technologies.

[7] N. Benvenuto and G. Cherubini, *Algorithms for Communications Systems and their Applications*, 4th ed. John Wiley & Sons, Jan. 2005.

[8] S. M. Kay, *Fundamentals of Statistical Signal Processing: Estimation Theory*. Prentice-Hall, 1993.

[9] C. Hofmann, K.-U. Storek, R. Schwarz, and A. Knopp, "Spatial MIMO over Satellite: A Proof of Concept," in *International Conference on Communications (ICC 2016), 2016 IEEE*, accepted for publication.

[10] P. Kyritsi, R. Valenzuela, and D. Cox, "Channel and capacity estimation errors," *Communications Letters, IEEE*, vol. 6, no. 12, pp. 517–519, Dec 2002.